Positron scattering from C_{20}

Ralph Carey and Robert R. Lucchese
Department of Chemistry, Texas A&M University, College Station, Texas 77843-3255, USA

F. A. Gianturco
Department of Chemistry, University of Rome "La Sapienza" and CNISM, Piazzale A. Moro 5, 00185 Rome, Italy
(Received 20 June 2007; revised manuscript received 22 April 2008; published 21 July 2008)

Ab initio calculations of 0.01–10 eV collisions of positrons with fullerene C_{20} are performed using a single-center expansion of the total wave function and a model potential to represent the positron-molecule interaction. Total elastic cross sections and eigenphase sums are generated and analyzed, while bound states and possible long-lifetime scattering resonances are explored, particularly those which are found to reside within the cage structure defined by the carbon atoms of the cluster.

DOI: 10.1103/PhysRevA.78.012706 PACS number(s): 34.80.Uv

I. INTRODUCTION

Fullerenes are a class of closed polyhedral carbon clusters C_n, characterized by a truncated icosahedral structure consisting of pentagonal and hexagonal faces among n carbon vertices [1]. Consisting only of pentagonal faces, the smallest fullerene believed to exist is C_{20} [2]. Unlike the larger C_{60}, icosahedral C_{20} has an electronic structure with an unfilled g orbital, so the cage suffers Jahn-Teller distortion that leads to a lower symmetry equilibrium structure [3–5].

Theoretical investigation of the structure of C_{20} have mostly attempted to distinguish energy levels among several structural conformations, from fullerene "cage" and corannulene "bowl," to rings and monocyclic chains [3,6–21]. The results vary widely with the level of theory, as tabulated by Sokolova *et al.* [15]. Although the cage has been calculated to be among the lowest in total energy, particularly among the density-functional theory (DFT) and post-Hartree-Fock methods [3,14], due to the highly strained geometry of fullerene C_{20} caused by its violation of the "isolated pentagon rule" [2], a few significant reports [22,23] have cast doubt on its very existence.

Until fairly recently, the lack of experimental evidence of fullerene C_{20} has supported the conclusion that it does not exist as a stable structure [10]. Additionally, experimental observation of C_{20} ions created by graphite vaporization shows monocyclic rings as the dominant structure [22] and subsequent DFT computations have confirmed that rings comprise the predominant products of graphite laser ablation [24]. Raman spectra of isolated C_{16}, C_{18}, and C_{20} clusters indicate that all three have the same type of geometry, which immediately rules out the corannulene bowl and fullerene cage as possible isomers [25]. Using Car-Parrinello molecular dynamics simulations, Brabec *et al.* [26] have proposed that C_{20} rings form in preference lower-energy cages, while going to bowl isomers with increasing temperature.

On the other hand, the mass spectra of the clusters evaporated from carbon nanotubes suggest the formation of cationic fullerene C_{20}^+ and not chains or rings [27]. The question of the existence of gas-phase fullerene C_{20}, however, was not settled until Prinzbach and co-workers [28] pioneered its synthesis from dodecahedrane ($C_{20}H_{20}$). The photoelectron spectrum of the fullerene anion C_{20}^-, shows an electron affinity of 2.25 eV and a vibrational progression of 730 cm^{-1}. Saito and Miyamoto [29], in their hybrid time-dependent DFT calculation, found an electron affinity of 2.86 eV and an overall agreement with the experimental spectrum. At nearly the same time as the first synthesis of the gas-phase fullerene, the molecular solid dodecahedral *fullerite* C_{20} has been synthesized from Ar^+ ion irradiation of high molecular weight polyethylene [30]. Iqbal *et al.* [31], under radically different conditions, have synthesized the solid from UV laser ablation of thin diamondlike carbon films. Considerable interest lies in the fullerite because of predictions that different phases may be either semiconductors or superconductors [32].

Many of the properties of fullerene C_{20} beyond geometric optimization, reviewed in depth by Orden and Saykally [23] and Lu and Chen [33], have been obtained only theoretically. These include computations of the polarizability of the series of fullerene clusters [34], with the C_{20} isomer constrained to the icosahedral (I_h) point group, the first ionization potential [35], and the vibrational spectrum [36,37]. Therefore, in the case of electron, photon, and, particularly, the positron physics that forms the basis of this report, much of the discussion will compare results obtained here to the theoretically [38] and experimentally [39] better-characterized fullerene C_{60}. We will very briefly state below the results relevant for the present discussion.

In addition to having a low electron affinity of nearly 2.7 eV [40,41], numerous electron attachment experiments have confirmed the existence of long-lived anionic metastable states in gas-phase C_{60} [42–44], during which almost no vibrational excitation takes place [45]. Inelastic electron scattering cross sections of the gas-phase fullerene show many of the same features as the solid, with the band shifts due primarily to the collective vibrations of the latter [46]. The similarity of the valence photoelectron spectra of thin-film C_{60} to that of the gas phase has been noted as well [47].

Photophysical processes of C_{60} have received less attention [48]: Berkowitz [49] has constructed the absolute photoabsorption cross spectrum of C_{60} from the patchwork of available relative and absolute experiments, while Becker and co-workers have performed a series of photoelectron angular distribution measurements over a range of photon en-

 ©2008 The American Physical Society

ergies [50–52], noting not only similar photoelectron spectra of the gas phase to the solid phase [53], but also the origin of the photoionization cross section oscillations of the highest occupied molecular orbitals (HOMO), specifically, quantum interference of the photoelectron wave functions from the nearly spherical target [51]. Subsequent theories using more elaborate representations of the fullerene target have verified this explanation [54,55].

Experiments on the simplest electron-molecule process, elastic scattering, have been performed only at high energy, in which the Born approximation is appropriate [56]. To the best of our knowledge, the only results on low-energy electron scattering from gas-phase C_{60} are those of Tanaka *et al.* [57], which report differential cross sections between 30° and 90° at selected energies.

Relevant experimental [58–62] and theoretical [63,64] positron-fullerene studies are limited primarily to annihilation dynamics in fullerites. Most experiments have found a positron lifetime in solid C_{60} near 400 ps, greater than that of other carbon phases such as graphite, diamond, or condensed-phase benzene [59,63]. Furthermore, due to pressure dependence of the lifetime, most researchers have concluded that positron density accumulates within the hexagonal interstices of the crystal lattice [62], not the molecular fullerenes themselves. To date, no elastic positron scattering results from either fullerenes or fullerites have been published.

Theoretical studies of the photophysics of the fullerenes, including C_{20} through C_{60} and beyond, primarily made use of simplified models such as the spherical jellium model [65–67] to simulate the extensive carbon network. Amusia *et al.* [68] have calculated photoionization cross sections using a simple spherical δ-function potential. Yu and collaborators [51] used a more sophisticated, multiparameter spherical-well approximation of the C_{60} fullerene cage. On the other hand, Decleva and co-workers [55,69,70], in their study of the photoemission spectra of C_{60}, have avoided jellium approximations in favor of a single-center expansion of the fullerene orbitals computed under the local-density approximation (LDA) Hamiltonian; Saito and Miyamoto [29] optimized neutral and anionic C_{20} at the Becke-Lee-Yang-Parr (BLYP) 6-311G* level. Lima *et al.* have computed the elastic electron-scattering cross sections of C_{60}, in addition to several large hydrocarbons, with a Monte Carlo adapted optical model [71]. To date, however, the highest-level electron- and positron-scattering calculations of fullerene targets have been those of Gianturco and collaborators [72–78] and, recently, Winstead and McKoy [79], who applied multichannel approaches to *ab initio* and to semiempirical (spherical well) fullerene C_{60} models to obtain integral and differential elastic electron-scattering cross sections.

Winstead and McKoy [79] note that their computation at the level of exact exchange (SE) results in resonance energies that are uniformly too high. Accordingly, they shift their results down by roughly 2–3 eV not only to align the lowest-energy resonances to the known anionic bound states of solid- and gas-phase C_{60}, but also to account for the correlation and polarization interactions neglected by the SE approximation. The energies and symmetries of their shifted resonances correspond approximately to those of Gianturco and collaborators [72–74], whose calculations explicitly include correlation and polarization through one-electron model potentials. On the other hand, the energies of the bound states and lowest-energy resonances of C_{60}, as reported in Lucchese *et al.* [66], result in resonance and bound state energies located consistently 0.6 eV above experiment. Similarly, in the valence photoemission of C_{60}, Becker and co-workers [52] note the overall agreement between their experimental cross sections and those of Decleva *et al.* [55] and Gianturco and Lucchese [78] for the lowest-energy occupied orbitals, even as features in both theoretical cross sections suggest shape resonances not detected in experiment.

Clearly, one of the ongoing issues in molecular scattering theory lies in the accurate computation of bound and resonant energies, which relies on a rigorous description of the electron- or positron-molecule interaction. In electron scattering, thorough *ab initio* procedures make use of multiconfigurational wave function descriptions of the target to account for electron correlation, and as recently noted [80] even this computationally expensive method fails to account for resonances due to core excitations unless the relevant configurations are explicitly included within the calculation. This difficulty lies at the heart of the present work, since the positron-molecule interaction is not as well understood as the electron-molecule interaction and, particularly, no model thus far has been provided to describe positron-scattering resonances, while none have been identified conclusively to date in positron-scattering studies from atoms or molecules.

In this report we consider partial and total integrated cross sections (ICSs) for positron-C_{20} scattering. These cross sections, in conjunction with the plots of the eigenphase sums and the computed poles of the analytic S matrix, provide evidence for the location of possible shape resonances originating during the scattering process. Bound states will also be considered in the present analysis.

II. THEORY

The theoretical basis for the present calculation is the same as that for cubane [81] and fullerene C_{60} [77]. We will therefore present a very brief outline of the methods used.

A. Single-center expansion

The wave functions of the bound electrons of the target $\phi_i^{p_i\mu_i}$ and of the impinging positron $\psi^{p\mu}$ are written in terms of a single-center expansion (SCE) located at the center of mass of the target, under the assumptions of the Born-Oppenheimer and fixed-nuclei approximations as follows:

$$\phi_i^{p_i\mu_i}(\mathbf{r}) = \frac{1}{r}\sum_{l,h} u_{ilh}^{p_i\mu_i}(r) X_{lh}^{p_i\mu_i}(\hat{r}), \tag{1}$$

$$\psi^{p\mu}(\mathbf{r}_p) = \frac{1}{r_p}\sum_{l,h} \psi_{lh}^{p\mu}(r_p) X_{lh}^{p\mu}(\hat{r}_p). \tag{2}$$

The label i refers to a specific orbital which belongs to the irreducible representation (IR) of the point group of the mol-

ecule. The index p refers to the relevant IR with μ indicating one of its components. The index h labels a specific angular basis function for a given partial wave l. The symmetry-adapted angular functions $X_{lh}^{p\mu}$ are defined in terms of the familiar spherical harmonics Y_{lm} by

$$X_{lh}^{p\mu}(\hat{r}) = \sum_{m} b_{lmh}^{p\mu} Y_{lm}(\hat{r}). \tag{3}$$

The details for the computation of the matrices $b_{lmh}^{p\mu}$ are found elsewhere [82]. We note that for the Abelian systems under consideration the label μ may be dropped.

If the positron-molecule interaction can be expressed in a purely local form V_{loc}, then the SCE results in the reduction of the three-dimensional scattering Schrödinger equation to a set of coupled radial ordinary differential equations

$$\left[\frac{d^2}{dr_p^2} - \frac{l(l+1)}{r_p^2} + k^2\right] \psi_{lh}^{p}(r_p) = 2 \sum_{l'h'} [V_{\text{loc},lh,l'h'}(r_p) \psi_{l'h'}^{p}(r_p)] \tag{4}$$

that are solvable using standard numerical techniques [83]. The solutions yield rotationally summed, integral elastic cross sections for each IR. Elements of the K matrix are obtained from fitting the solutions to the correct asymptotic form, namely [84],

$$\lim_{r_p \to \infty} \psi_{lh,l'h'}^{p} = \sin\left(kr_p - \frac{1}{2}l\pi\right)\delta_{ll'}\delta_{hh'} + K_{ij}^{p} \cos\left(kr_p - \frac{1}{2}l\pi\right), \tag{5}$$

which are related to the more familiar S matrix by

$$\mathbf{S} = \frac{\mathbf{I} + i\mathbf{K}}{\mathbf{I} - i\mathbf{K}}. \tag{6}$$

The local potential V_{loc} contains contributions from the dominant interactions between the positron and the molecular target,

$$V_{\text{loc}}(\mathbf{r}_p) = V_{\text{st}}(\mathbf{r}_p) + V_{\text{pcp}}(\mathbf{r}_p), \tag{7}$$

where V_{st} is the electrostatic potential between the positron and the molecular nuclei and electrons, while V_{pcp} combines the short-range correlation potential V_{corr} and long-range polarization potential V_{pol}.

B. Positron model

The correlation-polarization potential V_{pcp} consists of the sum

$$V_{\text{pcp}} = V_{\text{corr}} + V_{\text{pol}}. \tag{8}$$

The asymptotic polarization potential V_{pol} simply equals the lowest-order truncation of its second-order perturbation theory expansion

$$V_{\text{pol}} = -\sum_{l=1}^{\infty} \frac{\alpha_l}{2r_p^{2l+2}}. \tag{9}$$

To model the dominant short-range correlation interaction between the positron and the electrons of the target, we have used a DFT model, derived by Arponen and Pajanne [85], which assumes the positron is an isolated charged impurity interacting with an electron gas. Boronski and Nieminen [86] found the values of the correlation energy ε^{e-p} over all ranges of the electron density parameter r_s, which satisfies the relationship $\frac{4}{3}\pi r_s^3 \rho(\mathbf{r}) = 1$. That relationship between V_{corr} and ε^{e-p} is given by

$$V_{\text{corr}}(\mathbf{r}_p) = \frac{d}{d\rho}[\rho(\mathbf{r}_p)\varepsilon^{e-p}\rho(\mathbf{r}_p)], \tag{10}$$

where ρ denotes the undistorted electron density of the target. The full potential V_{pcp} consists of the piecewise-defined function matched at a distance r_p^c,

$$V_{\text{pcp}}(\mathbf{r}_p) = \begin{cases} V_{\text{corr}}^{\text{DFT}}(\mathbf{r}_p), & r_p \le r_p^c \\ V_{\text{pol}}(\mathbf{r}_p), & r_p > r_p^c, \end{cases} \tag{11}$$

the physical veracity of which is discussed in Lucchese *et al.* [87].

III. RESULTS AND DISCUSSION

As mentioned in the Introduction, neutral fullerene C_{20} is not a regular dodecahedron of symmetry I_h because of the Jahn-Teller distortion resulting from the degenerate electronic states arising from the partially filled molecular orbitals of its ground state [3]. In the majority of geometry optimizations the fullerene is found to belong to the low-symmetry point groups C_i or C_2, although occasionally higher-order point groups such as C_{2h} and D_{2h} have been obtained [33]. The recent work of Chen *et al.* [88] has demonstrated that the geometries of fullerenes in most nondihedral point groups are nearly isoenergetic. Nevertheless, the C_i and C_2 isomers were chosen because they represent the lowest-symmetry ground states consistent with the principles of Jahn-Teller distortion.

The ground state electronic configuration of C_{20} was optimized with the GAUSSIAN 03 [89] at the Becke three-parameter Lee-Yang-Parr D95* level of theory for isomers of both point groups. With 120 bound electrons, the C_i isomer has a SCF energy of −761.5279 a.u., an average bond length of 1.45 Å, and a molecular radius of 2.04 Å; the C_2 isomer has a SCF energy of −761.5298 a.u., and an average bond length of 1.45 Å and a molecular radius of 2.04 Å. Calculated isotropic polarizabilities of 171.56 and 171.55 a.u.^{3} for the respective C_i and C_2 isomers will be important in the discussion of the nature of the positron-target interaction potential.

The convergence parameters of the present SCE treatment are given as follows: for fullerenes of both point groups, the maximum orbital angular momentum for the expansion of the wave functions of the molecular orbitals and of the incident positron is limited to $l_{\text{max}}=40$. The summation over the optical and nuclear potentials is set to $2l_{\text{max}}$. The matching of the correlation V_{corr} and polarization V_{pol} potentials of V_{pcp} is done by explicitly placing a "polarizability center," 1/20th of the total isotropic polarizability, on each carbon nucleus. This results in a minor difference of 8.5780 a.u.^{3} and 8.5775 a.u.^{3} per carbon nucleus of the C_i and C_2 fullerene

isomers and imparts a nonspherical model of the full V_{pcp} of Eq. (11). The analytic matching radii r_p^c were, for the C_i and C_2 isomers, 5.6726 a.u. or 2.95 Å and 5.9780 a.u. or 3.11 Å, respectively.

A. Features of the adiabatic potentials

In addition to the symmetry-adapted angular basis set X_{lh}^p, the eigenfunctions obtained from diagonalizing the angular Hamiltonian at each radial distance r provide an alternative expansion basis set for the SCE. These distance-dependent, angular eigenstates Z_k^p, denoted adiabatic angular basis functions, are linear combinations of the previous angular basis set X_{lh}^p as follows:

$$Z_k^p(\mathbf{r}_p) = \sum_{lh} X_{lh}^p C_{lh,k}(r_p). \tag{12}$$

The expansion coefficients $C_{lh,k}$ are given by the matrix equation

$$\sum_{l'h'} V_{\mathrm{loc},lh,l'h',k}(r_p) C_{l'h',k}(r_p) = C_{lh,k}(r_p) V_k(r_p). \tag{13}$$

The eigenvalues V_k form the adiabatic potentials for each IR comprising the relevant point group of the target for each index value k, representing an "angular channel" (l,h), over the range of the positron-molecule distances. It can be shown [90] that solving the appropriate scattering equations using these adiabatic potentials can yield the same results for systems with purely local potentials given by the SCE method outlined previously. One of the advantages of using these potentials is that a single potential often is found responsible for the appearance of a given resonance. These potentials, therefore, allow the dominant features of the positron-molecule interaction to be seen qualitatively at a glance.

As shown in Figs. 1 and 2, only the $l=0$ radial potentials of the symmetric IRs A_g and A_u for the C_i and A,B for the C_2 point groups possess attractive regions within the framework of the carbon cage, which is located approximately 3.5 a.u. away from the center of mass at $r=0$. This potential barrier at the cage boundary is the result of the unique spatial features of C_{20}, as computed by V_{tot}, where the repulsive Coulombic potential and the attractive V_{pcp} meet. However, all adiabatic potentials with $l \leq 3$ further possess fairly substantial attractive wells, ranging from 3 to 8 eV just outside the cage. We should note that the exohedral positron-C_i fullerene potential wells are about 1.5 eV shallower than the corresponding inner wells formed by the C_2 cage, thereby indicating a more repulsive interaction between the positron and the C_i isomer outside the C atoms' network.

B. Features of the integrated cross sections

Unlike the positron cross section for C_{60}, which increases to some large finite value as the collision energy vanishes [77], the ICS for both isomers, as shown in Fig. 3, display strong near-threshold peaks, with a gradual, but not monotonic, decay at higher scattering energies. Comparing the present positron ICS to the electron total cross sections computed previously [72], the collision energies of the most

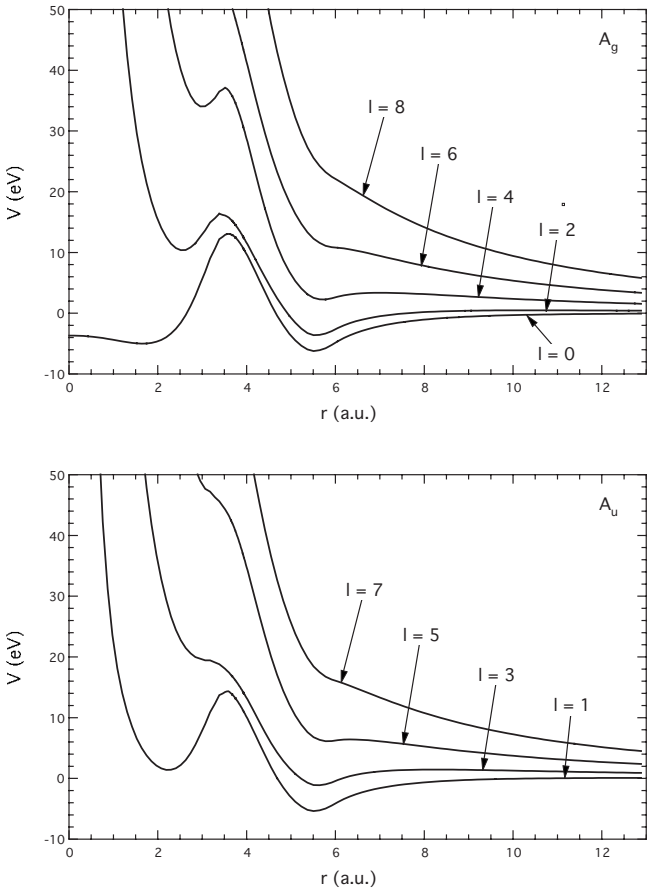

FIG. 1. Computed adiabatic potentials for the C_i structural isomer.

prominent peaks of both isomers are shifted to lower energy by about 2 eV. This is due to the stronger nature of the V_{pcp} potential at low collision energies, in contrast to the model electron correlation-polarization and exchange potentials discussed at length in Refs. [73,76]. However, at higher scattering energies, the positron ICSs display fewer of the structural features present in electron-scattering cross sections from the respective systems. This, too, is due to the Coulombic nuclear repulsion, which dominates the weakly attractive long-range polarization interaction in the case of positron scattering.

Partial cross sections were computed for each IR comprising the total point group of the fullerene cage, namely, A_g and A_u for the C_i isomer, shown in Fig. 4, and A and B for the C_2 isomer, shown in Fig. 5. In C_i, the symmetric IR contributes nearly two-thirds of the total scattering cross-section peak seen just under 1 eV. Furthermore, the broader peak around 5 eV is due exclusively to the A_g IR. The C_2 total cross section, displayed in the lower panel of Fig. 3, is plotted against the logarithm of the positron impact energy to better resolve the sharp, narrow double peaks at 0.1 eV. Similar to the C_i isomer, these sharp peaks are due to the symmetric IR (upper panel of Fig. 5) since the B partial cross section (Fig. 5, lower panel) rises to less than 160 Å^2 at its maximum. Other noted features of the C_2 total cross section include the broad peak seen near 1.3 eV and the comparatively small peak at 5 eV, both found in the A IR.

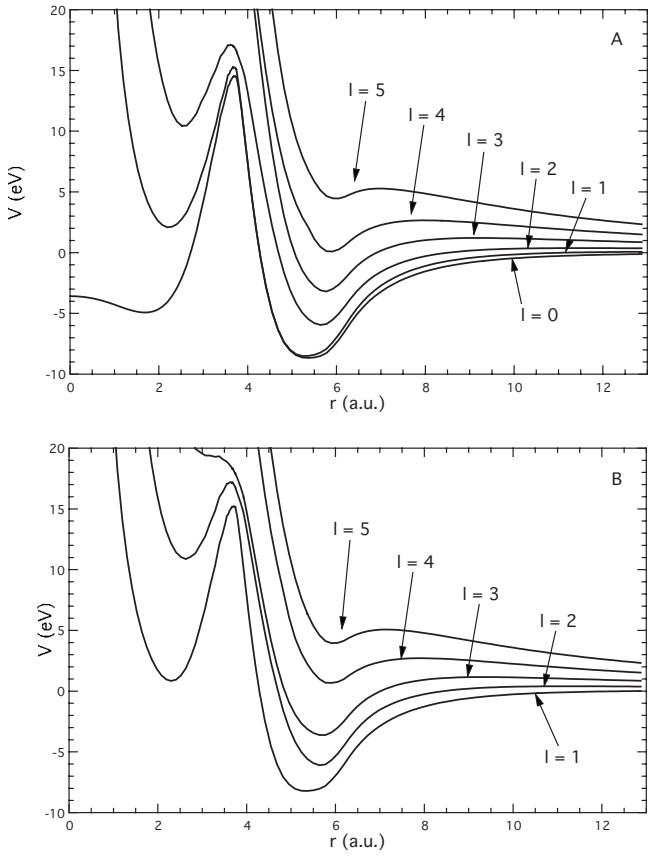

FIG. 2. Computed adiabatic potentials for the C_2 structural isomer.

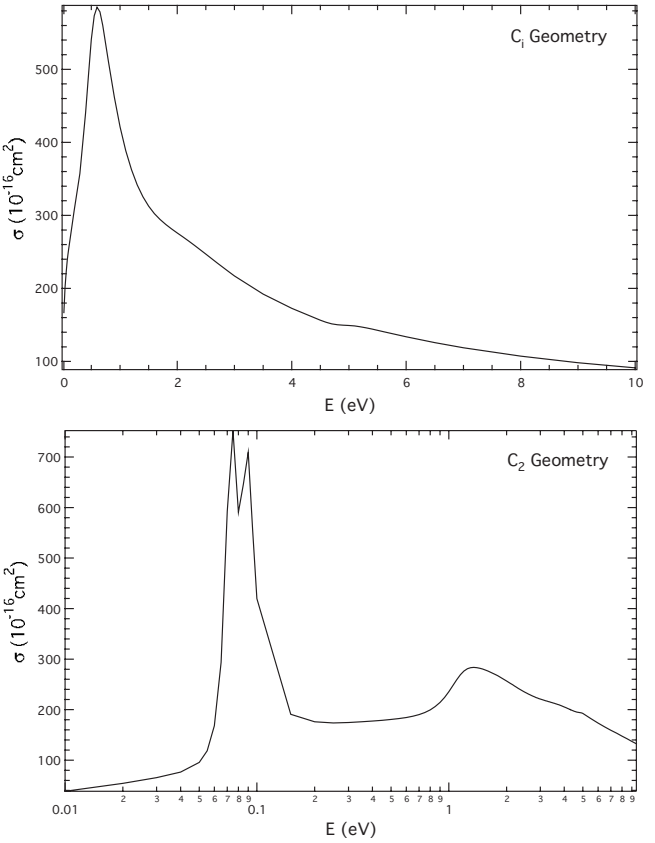

FIG. 3. Total positron-scattering cross sections for the C_{20} cage of C_i (upper panel) and C_2 (lower panel) geometries. Notice the different energy scales in the two panels.

C. Resonance properties

In resonant scattering calculations each isolated resonance of energy E_R, possessing a width Γ inversely proportional to its lifetime, is due to a pole at a complex energy $E=E_R-\frac{i}{2}\Gamma$ of the S matrix [91]. The matrix elements of $\mathbf{S}$ are obtained from solutions of Eq. (4) with the asymptotic form

$$\lim_{r_p\to\infty} \psi_{lh,l'h'}(r_p) = h_l^-(kr_p)\delta_{ll'}\delta_{hh'} - S_{lh,l'h'}h_l^+(kr_p), \quad (14)$$

where $h^{\pm}$ are spherical Hankel functions. Resonances occur at energies for which $\det \mathbf{S}^{-1}=0$. In general, the task of locating complex zeros of a complex-valued function is not trivial; a full account of the methodology to find the roots of the inverse S matrix may be found in Stratmann and Lucchese [92].

Although this procedure finds several poles for all IRs of both isomers—27 poles for the A and 25 for the B IRs for the C_2 isomeric cage alone, having real parts of the energy between 0 and 14 eV—only the ones whose widths Γ are small enough such that the corresponding poles in the S matrix lay reasonably close to the positive real axis were investigated further. In this case, somewhat arbitrarily, we have considered states with widths less than about 2 eV, which correspond to lifetimes τ of about 0.01 ps, according to the relation $\tau\sim\frac{\hbar}{\Gamma}$. Tables I and II list the energies, widths, and dominant asymptotic partial waves of the "physical" S-matrix poles of the C_i and C_2 isomeric cages, respectively.

In addition to the quantitative search for the roots of the inverse S matrix, resonances were also located by inspection of the eigenphase sums, as shown in Figs. 6 and 7. Ideally, the phase shift rises by π wherever the scattering energy moves across an isolated resonance, the position of which is determined at the energy for which $\delta_{\text{res}}=\frac{1}{2}\pi(\text{mod }\pi)$. Overlapping resonances induce a rapid rise by several π over the slowly rising background through a narrow energy region. Although no empirical fitting procedure such as the Breit-Wigner formula [93] was used to extract resonance properties from the phase sums directly, when analyzed in conjunction with the analytic search of poles of the S matrix, the eigenphase plots provide greater information on the positions of the energies of scattering resonances, particularly weak or broad ones, than that allowed from inspection of the integrated cross sections alone.

Shape resonances in electron scattering occur when electrons are trapped behind the potential barrier formed by the strongly attractive electron-molecule static potential and the centrifugal barrier associated with the angular momentum of the incoming electron. By contrast, the strongly repulsive interaction between the positron and the nuclei of the molecular target, combined with the centrifugal barrier, limits the angular momentum mechanisms in positron resonances to low angular momentum states. For example, in electron scattering from C_{20}, resonant states with angular momentum, including $l=8$, were found [73]. However, fullerene C_{20}, like

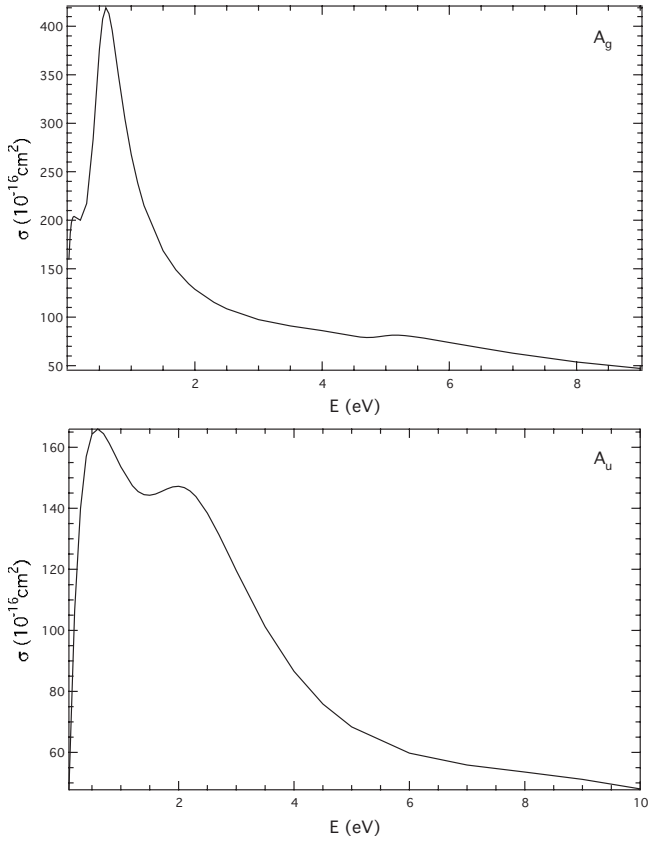

FIG. 4. Computed A_g (upper panel) and A_u (lower panel) partial cross sections for C_i cage geometry.

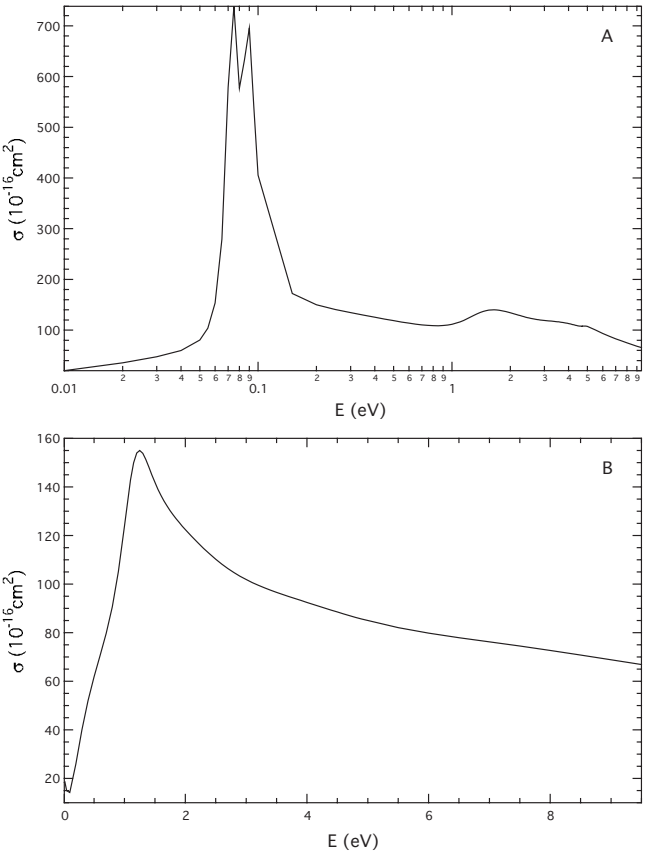

FIG. 5. Computed A (upper panel) and B (lower panel) partial cross sections for C_2 cage geometry.

C_{60}, has a large computed polarizability relative to its volume [94] and an absence of nuclear potential within the cage itself, thus leading to resonances trapped, as such, by the $l=0$ potential barrier. In addition, as suggested by the adiabatic potentials presented earlier in Figs. 1 and 2, positrons trapped by angular momentum barriers may appear for states $l \neq 0$ at low collision energies.

For the C_i isomer, the A_g eigenphase sum, displayed in the lower panel of Fig. 6, rises strongly near the scattering energy of 0.5 eV, and more slowly at 4.7 eV. The energies of these features in the eigenphase sums correspond well to the six narrow-width poles of the S matrix found for this system, as listed in Table I. Five poles were found in the region of the rising phase shift between 490 and 520 meV. These are in general long-lived $l=2$ scattering resonances that lie outside the carbon cage. However, the remaining pole, located at $E_R=4.80$ eV, $\Gamma=0.83$ eV, did yield an *encaged* s-wave positron resonance, the significance of which will be discussed below.

In contrast, the eigenphase sum of the antisymmetric A_u IR, seen in the lower panel of Fig. 6, is *decreasing* between 0 and 700 meV, a phenomenon that is in keeping with the presence of an entirely repulsive potential [91]. The analytic search of poles for this IR found seven short-lived $l=3$ resonances with energies between 1.39 and 1.50 eV, and are listed in Table I. In this case, the correlation between these seven poles and the eigenphase sum, which rises by only π over a falling background, is less explicit.

For the C_2 isomer, the A eigenphase sum shown in the upper panel of Fig. 7 rises sharply by 2π within a 0.3 eV energy range. It rises again, less steeply, between 1 and 2 eV, and further still between 4 and 5 eV. Four poles of the S matrix, reported in Table II, have real parts of their energies lying within the ranges of the features of the eigenphase shifts. Two poles with very low resonance energies, E_R

TABLE I. Resonant states of $e^+ + C_{20}$ in C_i geometry. Resonance energies E_R and widths Γ are in eV.

Cage geometry	IR	E_R	Γ	Partial wave
C_i	A_g	0.49	0.43	d
		0.49	0.43	d
		0.51	0.43	d
		0.51	0.44	d
		0.52	0.42	d
		4.80	0.83	s
	A_u	1.39	2.16	f
		1.47	2.31	f
		1.48	2.32	f
		1.50	2.32	f
		1.51	1.96	f
		1.60	2.04	f
		1.60	2.04	f

TABLE II. Resonant states of $e^+ + C_{20}$ in C_2 geometry. Resonance energies E_R and widths Γ are in eV.

Cage geometry	IR	E_R	Γ	Partial wave
C_2	A	0.06	0.01	d
		0.07	0.01	d
		1.26	0.84	d
		1.33	1.47	f
		4.80	0.92	s
	B	0.04	2.03	p,d,f
		1.07	0.70	d,f
		1.11	0.50	f
		1.39	1.77	f

=60 meV and E_R=70 meV, are long-lived d-wave resonances. Another pole, with energy E_R=1.26 eV, is a high orbital angular momentum f-wave resonance. The remaining resonance, at E_R=4.8 eV, Γ=0.92 eV, is an *encaged* s-wave resonance very close in energy, but somewhat broader in width, to that found for the A_g IR of the C_i isomer.

The eigenphase sum of the B IR in Fig. 7 shows a single narrow rise by approximately 4π for scattering energies near 1 eV. The B IR yields four S-matrix poles with energies lying within this region, as listed in Table II. Two long-lived resonances, one at E_R=1.07 eV and the other at E_R=1.11 eV,

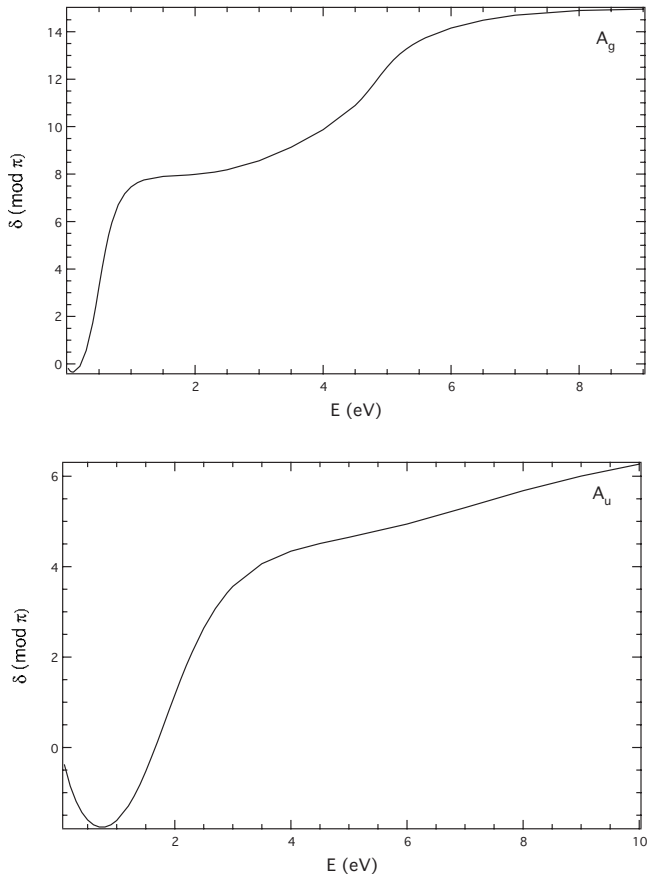

FIG. 6. Eigenphase sums for A_g (upper panel) and A_u (lower panel) IRs of C_i geometry.

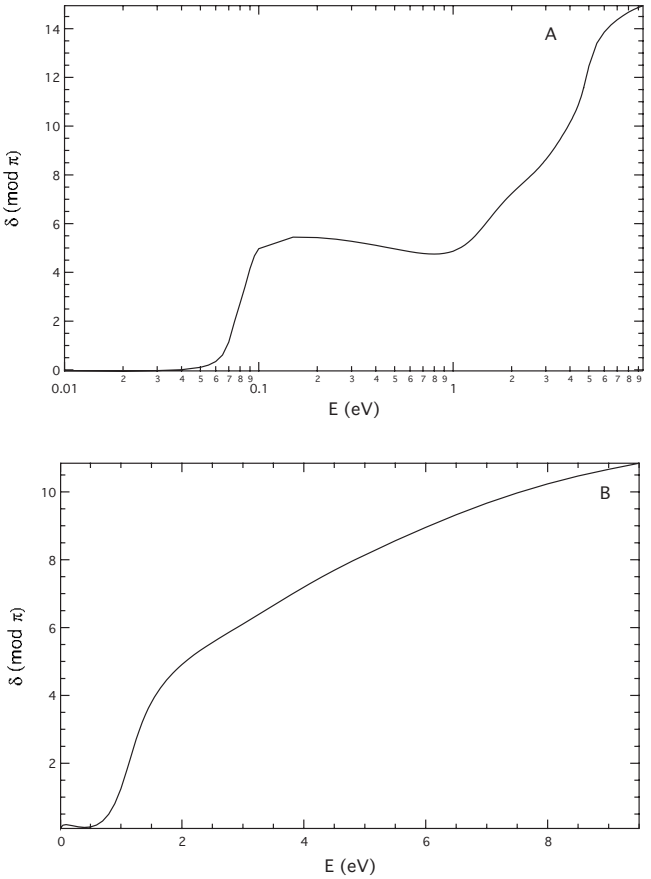

FIG. 7. Eigenphase sums for the A (upper panel) and B (lower panel) IRs for C_2.

have dominant f-wave components. One of the two shorter lifetime resonances has a very low resonant energy of E_R =40 meV and is predominantly of p-wave nature, while the other is a higher-energy (E_R=1.39) l=3 state.

The most remarkable feature of broad resonances in electron scattering is the possibility for the metastable electron to tunnel through a lower angular-momentum potential barrier coupled to it by the multichannel potential. This "leaking out" from a dominant higher partial wave through lower partial waves consequently leads to shorter lifetimes [73]. Such a mechanism does not appear to occur for the short-lived resonances found here. The B resonance wave at E_R =1.07 eV, in Table II, contains both l=2 and l=3 partial waves that does not appreciably reduce its lifetime as compared to the single-channel l=3 resonance at E_R=1.11 eV. In contrast, the lowest-energy B resonance of 40 meV contains three competing channels, the lowest of which, l=1, allows very rapid escape of the positron as reflected in its broad resonance width of 2.02 eV.

Computed three-dimensional wave functions of the s-wave resonances of both isomers in Fig. 8 clearly indicate that the majority of their probability amplitudes exist within the cavity of the fullerene cages. Although the lifetimes of these resonances are fairly short (approximately 0.07 ps for widths around 900 meV), the energies are not high enough to cause the fragmentation of the carbon network: how this relates to the positron dynamics of fullerene C_{20} remains un-

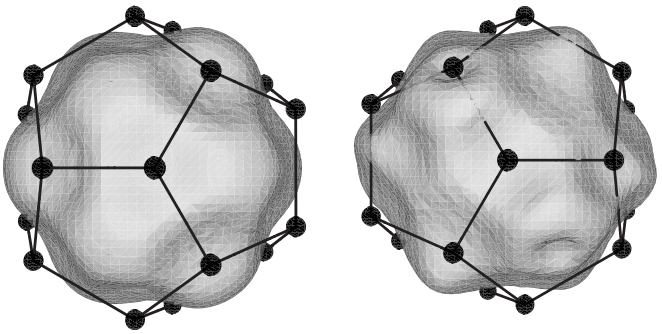

FIG. 8. Three-dimensional representations of the resonant orbitals localized within the C_i (left) and C_2 (right) cages.

clear. Experimental results do not support the hypothesis that positron density localizes within C_{60} fullerenes, as stated in the Introduction; therefore, it is even less likely that positron density should be found within the smaller C_{20} cage. However, among C_{60} fullerites, positron annihilation may occur within the cavity if heavy alkali atoms are used as dopants within the hexagonal interstices of the molecular crystal [62,95]. Thus, positron localization within the fullerene cage is certainly *possible,* particularly for fullerenes in the gas phase. Indeed, assuming that the $l=0$ adiabatic potentials of both isomers may be crudely represented as a square well of width $r=1$ a.u. and height $V=15$ eV at the cage boundary, and neglecting processes such as virtual positronium formation [96] not modeled in the present SCE, then the probability of the positron of resonance energy $E=4.8$ eV to tunnel through the repulsive cage barrier is a considerable 10% [97]. This result assumes that the lifetime of the computed resonance is less than the annihilation lifetime of positrons in C_{20}, for which no result, theoretical or experimental, has been published to date.

So-called "endohedral" A_g resonances are also seen in the C_{60} calculations of both Winstead and McKoy [79] and Gianturco and Lucchese [76]. The Schwinger multichannel calculation at the level of exact static exchange found an endohedral resonance lying at $E_R=3.2$ eV, $\Gamma=0.89$ eV, while the SCE found the equivalent resonance at $E_R=2.76$ eV, $\Gamma=0.52$ eV. Gianturco and Lucchese argue that this resonance results from the dynamical coupling of the $l=0$ to the $l=10$ partial waves, while Winstead and McKoy state that the A_g resonance corresponds to an anomalous ("non-σ, non-π") anion identified in the condensed molecular photoemission spectrum. Similarly, in their study on positron scattering from C_{60}, where they make use of a comparative electron correlation potential, Gianturco and Lucchese [77] found an encaged A_g positron resonance at 3.24 eV and a width of less than 0.01 eV. A similar calculation that uses the positron correlation potential of the present report finds the A_g resonance lowered in energy to yield a positronic bound state, i.e., the formation of C_{60}^+ by positron impact. Interestingly, investigation of the electron-scattering resonance on the C_2 isomer of C_{20} [73] yielded no resonant wave functions with significant probability density trapped within the cage.

At this point in the discussion, we should mention that our search for all physically meaningful poles of the S matrix yielded a number of bound states as well: they are listed by IR, energy, and dominant partial wave in Tables III and IV. The location along the negative real axis of the complex energy plane and the requirement that the wave function decay at asymptotic radial distances distinguish these bound states from that of resonant states discussed previously.

TABLE III. Bound states of $e^+ + C_{20}$ in C_i symmetry. Bound state energies E_B are in eV.

Cage geometry	IR	E_B	Partial wave
C_i	A_g	−0.78	s
	A_u	−0.25	p
		−0.23	p
		−0.23	p

The C_i isomer possesses four bound states (listed in Table III), among which the lowest in energy is an s-wave A_g bound state of −780 meV, while the remaining three are higher-energy A_u p-wave states between −250 and −220 meV. The probability maxima of all of these bound states lie near 6 a.u., outside the fullerene network. The C_2 fullerene cage has a larger array of bound states, listed in Table IV, that are not as well characterized by partial waves as those of the C_i isomer. While the A IR has two bound states, an s-wave state at −2.11 eV and a d-wave state at −370 meV, the B IR has four bound states consisting of multiple partial wave contributions. Two bound states with energies near −1.8 eV have p- and d-wave components, while those at energies −460 and −230 meV each have predominant p- and d- and minor f-wave components.

The depth of the adiabatic potential wells $l \leq 3$, shown in Figs. 1 and 2 at the junction of the asymptotic and correlation-polarization potentials of V_{loc}, allow for the formation of these bound states since no bound states arise with significant probability densities inside either isomeric cage. The majority of the bound states have probability maxima near 6 a.u.; that is, they are only slightly removed from the matching radii r_p^c of Eq. (11).

The large number of bound and resonant positron states found in the present work suggest that fullerene C_{20}, in both symmetries, is likely to support weak positron attachment, even under the assumption of the fixed-nuclei approximation whereby the nuclear geometry remains unchanged during the scattering event. This suggestion must be qualified by the fact that cation formation through positron attachment has

TABLE IV. Bound states of $e^+ + C_{20}$ in C_2 symmetry. Bound state energies E_B are in eV.

Cage geometry	IR	E_B	Partial wave
C_2	A	−2.10	s
		−0.37	d
	B	−1.90	p,d
		−1.84	p,d
		−0.47	p,d,f
		−0.22	p,d,f

been conclusively demonstrated only theoretically, and merely for atoms [98]. But the fact that all bound states, and all but one resonance for the two C_{20} isomers, are located outside the cage corroborates the result of positron annihilation experiments on C_{60} and C_{70} surveyed in the Introduction, which suggest that positron density accumulates mostly outside the fullerene C-atom network.

IV. CONCLUSIONS

We have reported the results of low-energy positron scattering from C_{20} using a DFT potential to model the interaction of a positron with a multielectron target. The motivation for this work lies not only in the identification of possible scattering resonances and bound states, but also in the question as to whether positrons may become localized within the fullerene C-atom network.

Model adiabatic potentials show that the interaction between the positron and the molecular cluster becomes strongly repulsive for all partial waves with $l>0$, with attractive regions for $l\leq 3$ located outside the cage. The depth of these wells supports a small number of bound states for positrons of low angular momenta, and resonances at higher angular momenta. These results are sensitive not only to the adiabatic and fixed-nuclei approximations of the SCE but also to the nature of the assumed interaction potential V_{loc}, a function which depends on a correlation model that treats the positron as an isolated positive point charge and neglects positronium formation. Both assumptions enhance the attractive nature of the present positron-molecule interaction, thereby increasing the depth of the adiabatic potentials and the number of the metastable states such potentials may support.

The conclusions obtained from this qualitative analysis agree with those obtained from computed integrated partial cross sections, eigenphase sums, and analytic search of physical roots of the inverse S matrix. The partial ICS and eigenphase sums show evidence of several scattering resonances for both low symmetry isomers. However, the probability maxima of the resonance radial wave functions indicate that the majority of these resonances, and all of the bound states, lie outside the framework of the carbon cage. In general, at least in elastic scattering, one of the results for our present study is that no energetic advantage appears to exist for positrons to localize within the fullerene cavity of the C_{20} cage, while significant resonant and bound states are found to exist on, and outside, the C-atom network.

ACKNOWLEDGMENTS

The financial support of the Italian Ministry for University and Research (MIUR), NATO Collaborative Research Grant No. 950552, and the Robert A. Welch Foundation of Houston, Texas, under Grant No. A-1020, are gratefully acknowledged.

[1] H. W. Kroto, J. R. Heath, S. C. O'Brien, and R. E. Smalley, Nature (London) **318**, 162 (1985).
[2] H. W. Kroto, Nature (London) **329**, 529 (1987).
[3] V. Parasuk and J. Almöf, Chem. Phys. Lett. **184**, 187 (1991).
[4] G. B. Adams, O. F. Sankey, J. B. Page, and M. O'Keeffe, Chem. Phys. **176**, 61 (1993).
[5] B. L. Zhang, C. Z. Wang, K. W. Ho, C. H. Xu, and C. T. Chan, J. Chem. Phys. **97**, 5007 (1992); C. Z. Wang, B. L. Zhang, K. M. Ho, and X. Q. Wang, Int. J. Mod. Phys. B **7**, 4305 (1993).
[6] K. Raghavachari, D. L. Strout, G. K. Odom, G. E. Scuseria, J. A. Pople, B. G. Johnson, and P. M. W. Gill, Chem. Phys. Lett. **214**, 357 (1993).
[7] M. Sawtarie, M. Menon, and K. R. Subbaswamy, Phys. Rev. B **49**, 7739 (1994).
[8] H. Handschuh, G. Gantefor, B. Kessler, P. S. Bechthold, and W. Eberhardt, Phys. Rev. Lett. **74**, 1095 (1995).
[9] P. R. Taylor, E. Bylaska, J. H. Weare, and R. Kawai, Chem. Phys. Lett. **235**, 558 (1995).
[10] J. C. Grossman, L. Mitas, and K. Raghavachari, Phys. Rev. Lett. **75**, 3870 (1995).
[11] Z. Q. Wang, P. Day, and R. Pachter, Chem. Phys. Lett. **248**, 121 (1996).
[12] J. M. L. Martin, J. ElYazel, and J. P. Francois, Chem. Phys. Lett. **248**, 345 (1996).
[13] E. J. Bylaska, P. R. Taylor, R. Kawai, and J. H. Weare, J. Phys. Chem. **100**, 6966 (1996).
[14] M. C. Domene, P. W. Fowler, D. Mitchell, G. Seifert, and F. Zerbetto, J. Phys. Chem. A **101**, 8339 (1997).
[15] S. Sokolova, A. Lüchow, and J. B. Anderson, Chem. Phys. Lett. **323**, 229 (2000).
[16] Cao Ze-Xian, Chin. Phys. Lett. **18**, 1060 (2001).
[17] S. Grimme and C. Muck-Lichtenfeld, ChemPhysChem **3**, 207 (2002).
[18] K. R. Greene and K. A. Beran, J. Comput. Chem. **23**, 938 (2002).
[19] C. J. Zhang, X. Xu, and Q. M. Zhang, Chem. Phys. Lett. **364**, 213 (2002).
[20] Z. F. Chen and W. Thiel, Chem. Phys. Lett. **367**, 15 (2003).
[21] W. An, Y. Gao, S. Bulusu, and X. C. Zeng, J. Chem. Phys. **122**, 204109 (2005).
[22] G. von Helden, M. T. Hsu, N. G. Gotts, P. R. Kemper, and M. T. Bowers, Chem. Phys. Lett. **204**, 15 (1993).
[23] A. Van Orden and R. J. Saykally, Chem. Rev. (Washington, D.C.) **98**, 2313 (1998).
[24] J. Lu, S. Re, Y. Choe, S. Nagase, Y. Zhou, R. Han, L. Peng, X. Zhang, and X. Zhao, Phys. Rev. B **67**, 125415 (2003).
[25] A. K. Ott, G. A. Rechtsteiner, C. Felix, O. Hampe, M. F. Jarrold, R. P. Van Duyne, and K. Raghavachari, J. Chem. Phys. **109**, 9652 (1998).
[26] C. J. Brabec, E. B. Anderson, B. N. Davidson, S. A. Kajihara, Q. M. Zhang, J. Bernholc, and D. Tomanek, Phys. Rev. B **46**, 7326 (1992).
[27] K. Hata, M. Ariff, K. Tohji, and Y. Saito, Chem. Phys. Lett. **308**, 343 (1999).

[28] H. Prinzbach, A. Weller, P. Landenberger, F. Wahl, J. Wörth, L. T. Scott, W. Gelmont, D. Olevano, and B. von Issendorff, Nature (London) **407**, 60 (2000); H. Prinzbach, A. Weller, P. Landenberger, F. Wahl, J. Wörth, L. T. Scott, W. Gelmont, D. Olevano, F. Sommer, and B. von Issendorff, Chem.-Eur. J. **12**, 6268 (2006).
[29] M. Saito and Y. Miyamoto, Phys. Rev. Lett. **87**, 035503 (2001).
[30] Z. X. Wang, X. Z. Ke, Z. Y. Zhu, F. Y. Zhu, M. L. Ruan, H. Chen, R. B. Huang, and L. S. Zheng, Phys. Lett. A **280**, 351 (2001).
[31] Z. Iqbal, Y. Zhang, H. Grebel, S. Vijayalakshmi, A. Lahamer, G. Benedek, W. Bernasconi, J. Cariboni, I. Spagnolatti, R. Sharma, F. J. Owens, M. E. Kozlov, K. V. Rao, and M. Muhammed, Eur. Phys. J. D **31**, 509 (2003).
[32] S. Okada, Y. Miyamoto, and M. Saito, Phys. Rev. B **64**, 245405 (2001); Y. Miyamoto and M. Saito, *ibid.* **63**, 161401(R) (2001).
[33] X. Lu and Z. Chen, Chem. Rev. (Washington, D.C.) **105**, 3643 (2005).
[34] B. Shanker and J. Applequist, J. Phys. Chem. **98**, 6486 (1994).
[35] G. Seifert, K. Vietze, and R. Schmidt, J. Phys. B **29**, 5183 (1996).
[36] G. Galli, F. Gygi, and J. Christophe Golaz, Phys. Rev. B **57**, 1860 (1998).
[37] M. Saito and Y. Miyamoto, Phys. Rev. B **65**, 165434 (2002).
[38] G. E. Scuseria, Chem. Phys. Lett. **176**, 423 (1991).
[39] K. Hedberg, L. Hedberg, D. S. Bethune, C. A. Brown, H. C. Dorn, R. D. Johnson, and M. de Vries, Science **254**, 410 (1991).
[40] S. H. Yang, C. L. Pettiette, J. Conceicao, O. Cheshnovsky, and R. E. Smalley, Chem. Phys. Lett. **139**, 233 (1987).
[41] A. G. Wang, J. Conceicao, C. M. Jin, and R. E. Smalley, Chem. Phys. Lett. **182**, 5 (1991).
[42] M. Lezius, P. Scheier, and T. D. Märk, Chem. Phys. Lett. **203**, 232 (1993).
[43] T. Jaffke, E. Illenberger, M. Lezius, S. Matejcik, D. Smith, and T. Märk, Chem. Phys. Lett. **226**, 213 (1994).
[44] S. Matejcik, T. D. Märk, P. Spanel, and D. Smith, J. Chem. Phys. **102**, 2516 (1995).
[45] O. Elhamidi, J. Pommier, and R. Abouaf, J. Phys. B **30**, 4633 (1997).
[46] J. W. Keller and M. A. Coplan, Chem. Phys. Lett. **193**, 89 (1992).
[47] D. L. Lichtenberger, L. W. Nebesny, C. D. Ray, D. R. Huffman, and L. Lamb, Chem. Phys. Lett. **176**, 203 (1991).
[48] U. Becker, O. Gessner, and A. Rudel, J. Electron Spectrosc. Relat. Phenom. **108**, 189 (2000).
[49] J. Berkowitz, J. Chem. Phys. **111**, 1446 (1999).
[50] T. Liebsch, O. Plotzke, F. Heiser, U. Hergenhahn, O. Hemmers, R. Wehlitz, J. Viefhaus, B. Langer, S. B. Whitfield, and U. Becker, Phys. Rev. A **52**, 457 (1995).
[51] Y. B. Xu, M. Q. Tan, and U. Becker, Phys. Rev. Lett. **76**, 3538 (1996).
[52] S. Korica, D. Rolles, A. Reinkoster, B. Langer, J. Viefhaus, S. Cvejanovic, and U. Becker, Phys. Rev. A **71**, 013203 (2005).
[53] P. J. Benning, D. M. Poirier, N. Troullier, J. L. Martins, J. H. Weaver, R. E. Haufler, L. P. F. Chibante, and R. E. Smalley, Phys. Rev. B **44**, 1962 (1991).
[54] S. Hasegawa, T. Miyamae, K. Yakushi, H. Inokuchi, K. Seki, and N. Ueno, Phys. Rev. B **58**, 4927 (1998).
[55] P. Decleva, S. Furlan, G. Fronzoni, and W. Stener, Chem. Phys. Lett. **348**, 363 (2001).
[56] L. G. Gerchikov, P. V. Efimov, V. M. Mikoushkin, and A. V. Solovyov, Phys. Rev. Lett. **81**, 2707 (1998).
[57] H. Tanaka, L. Boesten, K. Onda, and O. Ohashi, J. Phys. Soc. Jpn. **63**, 485 (1994).
[58] T. Azuma, H. Saito, and Y. Yamakazi, J. Phys. Soc. Jpn. **60**, 2812 (1991).
[59] H. E. Schaefer, M. Forster, R. Wurschum, W. Kratschmer, and D. R. Huffman, Phys. Rev. B **45**, 12164 (1992).
[60] Y. C. Jean, X. Lu, Y. Lou, A. Bharathi, C. S. Sundar, Y. Lyu, P. H. Hor, and C. W. Chu, Phys. Rev. B **45**, 12126 (1992).
[61] Y. Ito and T. Suzuki, Phys. Rev. B **60**, 15636 (1999).
[62] Y. Ito, Y. Iwasa, N. M. Tuan, and S. Moriyama, J. Chem. Phys. **115**, 4787 (2001).
[63] M. J. Puska and R. M. Nieminen, J. Phys.: Condens. Matter **4**, L149 (1992).
[64] S. Ishibashi, N. Terada, M. Tokumoto, N. Kinoshita, and H. Ihara, J. Phys.: Condens. Matter **4**, L169 (1992).
[65] V. K. Ivanov, G. Y. Kashenock, R. G. Polozkov, and A. V. Solov'yov, J. Phys. B **34**, L669 (2001); J. Exp. Theor. Phys. **96**, 658 (2003).
[66] A. Rudel, R. Hentges, U. Becker, H. S. Chakraborty, M. E. Madjet, and J. M. Rost, Phys. Rev. Lett. **89**, 125503 (2002).
[67] K. Yabana and G. F. Bertsch, J. Chem. Phys. **100**, 5580 (1994).
[68] M. Y. Amusia, A. S. Baltenkov, and B. G. Krakov, Phys. Lett. A **243**, 99 (1998).
[69] M. Venuti, W. Stener, G. De Alti, and P. Decleva, J. Chem. Phys. **111**, 4589 (1999).
[70] P. Colavita, G. De Alti, G. Fronzoni, W. Stener, and P. Decleva, Phys. Chem. Chem. Phys. **3**, 4481 (2001).
[71] L. G. Ferreira, A. R. Lopes, M. A. P. Lima, and M. H. F. Bettega, J. Phys. B **39**, 1045 (2006).
[72] F. A. Gianturco, G. Y. Kashenock, R. R. Lucchese, and N. Sanna, J. Chem. Phys. **116**, 2811 (2002).
[73] F. A. Gianturco, R. R. Lucchese, and N. Sanna, J. Chem. Phys. **118**, 4013 (2003).
[74] F. A. Gianturco, R. R. Lucchese, and N. Sanna, J. Phys. B **32**, 2181 (1999).
[75] R. R. Lucchese, F. A. Gianturco, and N. Sanna, Chem. Phys. Lett. **305**, 413 (1999).
[76] F. A. Gianturco and R. R. Lucchese, J. Chem. Phys. **111**, 6769 (1999).
[77] F. A. Gianturco and R. R. Lucchese, Phys. Rev. A **60**, 4567 (1999).
[78] F. A. Gianturco and R. R. Lucchese, Phys. Rev. A **64**, 032706 (2001).
[79] C. Winstead and V. McKoy, Phys. Rev. A **73**, 012711 (2006).
[80] C. Winstead and V. McKoy, Phys. Rev. Lett. **98**, 113201 (2007).
[81] F. A. Gianturco, P. Nichols, T. L. Gibson, and R. R. Lucchese, Phys. Rev. A **72**, 032724 (2005).
[82] F. A. Gianturco and A. Jain, Phys. Rep. **143**, 347 (1986).
[83] W. H. Press, B. P. Flannery, S. A. Teukolsky, and W. T. Vetterling, *Numerical Recipes. The Art of Scientific Computing* (Cambridge University Press, Cambridge, 1996).
[84] F. A. Gianturco, D. G. Thompson, and A. Jain, in *Computational Methods for Electron-Molecule Collisions*, edited by W.

Huo and F. A. Gianturco (Plenum, New York, 1995), p. 75.
[85] J. Arponen and E. Pajanne, Ann. Phys. (N.Y.) **91**, 450 (1975); **121**, 343 (1979).
[86] E. Boronski and R. M. Nieminen, Phys. Rev. B **34**, 3820 (1986).
[87] R. R. Lucchese, F. A. Gianturco, P. Nichols, and T. L. Gibson, in *New Directions in Antimatter Chemistry and Physics*, edited by C. M. Surko and F. A. Gianturco (Kluwer, Dordrecht, The Netherlands, 2001), p. 475.
[88] Z. F. Chen, T. Heine, H. J. Jiao, A. Hirsch, W. Thiel, and P. V. R. Schleyer, Chem.-Eur. J. **10**, 963 (2004).
[89] M. J. Frisch, G. W. Trucks, H. B. Schlegel, G. E. Scuseria, M. A. Robb, J. R. Cheeseman, J. Montgomery, J. A. T. Vreven, K. N. Kudin, J. C. Burant, J. M. Millam, S. S. Iyengar, J. Tomasi, V. Barone, B. Mennucci, M. Cossi, G. Scalmani, N. Rega, G. A. Petersson, H. Nakatsuji, M. Hada, M. Ehara, K. Toyota, R. Fukuda, J. Hasegawa, M. Ishida, T. Nakajima, Y. Honda, O. Kitao, H. Nakai, M. Klene, X. Li, J. E. Knox, H. P. Hratchian, J. B. Cross, V. Bakken, C. Adamo, J. Jaramillo, R. Gomperts, R. E. Stratmann, O. Yazyev, A. J. Austin, R. Cammi, C. Pomelli, J. W. Ochterski, P. Y. Ayala, K. Morokuma, G. A. Voth, P. Salvador, J. J. Dannenberg, V. G. Zakrzewski, S. Dapprich, A. D. Daniels, M. C. Strain, O. Farkas, D. K. Malick, A. D. Rabuck, K. Raghavachari, J. B. Foresman, J. V. Ortiz, Q. Cui, A. G. Baboul, S. Clifford, J. Cioslowski, B. B. Stefanov, G. Liu, A. Liashenko, P. Piskorz, I. Komaromi, R. L. Martin, D. J. Fox, T. Keith, M. A. Al-Laham, C. Y. Peng, A. Nanayakkara, M. Challacombe, P. M. W. Gill, B. Johnson, W. Chen, M. W. Wong, C. Gonzalez, and J. A. Pople, GAUSSIAN 03 (Gaussian, Inc., Wallingford, CT, 2004).
[90] R. R. Lucchese and F. A. Gianturco, Int. Rev. Phys. Chem. **15**, 429 (1996).
[91] R. Taylor, *Scattering Theory* (Wiley, New York, 1979).
[92] R. Stratmann and R. Lucchese, J. Chem. Phys. **97**, 6384 (1992).
[93] L. Landau and E. M. Lifshitz, *Quantum Mechanics: Non-Relativistic Theory* (Butterworth-Heinemann, Oxford, 2003).
[94] G. K. Gueorguiev, J. M. Pacheco, and D. Tomanek, Phys. Rev. Lett. **92**, 215501 (2004).
[95] Y. Lou, X. Lu, G. H. Dai, W. Y. Ching, Y. N. Xu, M. Z. Huang, P. K. Tseng, Y. C. Jean, R. L. Meng, P. H. Hor, and C. W. Chu, Phys. Rev. B **46**, 2644 (1992).
[96] D. M. Schrader and J. Moxom, in *New Directions in Antimatter Chemistry and Physics*, edited by C. M. Surko and F. A. Gianturco (Kluwer, Dordrecht, The Netherlands, 2001), p. 263.
[97] E. Merzbacher, *Quantum Mechanics* (Wiley, New York, 1998).
[98] J. Mitroy, M. W. Bromley, and G. G. Ryzhikh, J. Phys. B **35**, R81 (2002).